


Review

# Recent Advances in Gold Nanomaterials for Photothermal Therapy

Yao-Chen Chuang<sup>1,2</sup> , Hsin-Lun Lee<sup>1</sup>, Jeng-Fong Chiou<sup>1</sup> and Leu-Wei Lo<sup>2,\*</sup>

<sup>1</sup> Department of Radiation Oncology, Taipei Medical University Hospital, Taipei 110, Taiwan; 215123@h.tmu.edu.tw (Y.-C.C.); b001089024@tmu.edu.tw (H.-L.L.); solomanc@tmu.edu.tw (J.-F.C.)

<sup>2</sup> Institute of Biomedical Engineering and Nanomedicine, National Health Research Institutes, Zhunan 350, Taiwan

\* Correspondence: lwlo@nhri.edu.tw; Tel.: +886-37-246166 (ext. 37115)

**Abstract:** Gold nanoparticle (AuNPs)-mediated photothermal therapy (PTT) has attracted increasing attention both in laboratory research and clinical applications. Due to its easily-tuned properties of irradiation light and inside-out hyperthermia ability, it has demonstrated clear advantages in cancer therapy over conventional thermal ablation. Despite this great advancement, the therapeutic efficacy of AuNPs mediated PTT in tumor treatment remains compromised by several obstacles, including low photothermal conversion efficiency, tissue penetration limitation of excitation light, and inherent non-specificity. In view of the rapid development of AuNPs mediated PTT, we present an in-depth review of major breakthroughs in the advanced development of gold nanomaterials for PTT, with emphasis on those from 2010 to date. In particular, the current state of knowledge for AuNPs based photothermal agents within a paradigm of key structure-optical property relationships is presented in order to provide guidance for the design of novel AuNP based photothermal agents to meet necessary functional requirements in specific applications. Furthermore, potential challenges and future development of AuNP mediated PTT are also elucidated for clinical translation. It is expected that AuNP mediated PTT will soon constitute a markedly promising avenue in the treatment of cancer.

**Keywords:** gold nanomaterials; photothermal therapy; near infrared; thermal ablation; inside-out hyperthermia



**Citation:** Chuang, Y.-C.; Lee, H.-L.; Chiou, J.-F.; Lo, L.-W. Recent Advances in Gold Nanomaterials for Photothermal Therapy. *J. Nanotheranostics* **2022**, *3*, 117–131. <https://doi.org/10.3390/jnt3020008>

Academic Editor: Moein Moghimi

Received: 5 April 2022

Accepted: 23 May 2022

Published: 1 June 2022

**Publisher's Note:** MDPI stays neutral with regard to jurisdictional claims in published maps and institutional affiliations.



**Copyright:** © 2022 by the authors. Licensee MDPI, Basel, Switzerland. This article is an open access article distributed under the terms and conditions of the Creative Commons Attribution (CC BY) license (<https://creativecommons.org/licenses/by/4.0/>).

## 1. Introduction

Globally, cancer is the first- or second-leading cause of death. In recent decades, worldwide cancer incidence and mortality rates have been continuously increasing. According to estimates from the International Agency for Research on Cancer (IARC), 19.3 million new cancer cases (18.1 million, excluding nonmelanoma skin cancer) and almost 10.0 million cancer deaths (9.9 million, excluding nonmelanoma skin cancer) occurred in 2020 [1,2]. The growing knowledge of cancer biology, however, has facilitated the development of novel strategies to treat this disease. Thus far, surgery for the removal of tumor tissue followed by radiation therapy (RT) and chemotherapy are still the most recommended conventional cancer treatment strategies in the clinic, although these strategies suffer from the limitations of their nonspecific effects on nearby healthy tissues and manifold undesirable side effects [3–5]. These conventional therapies are also incapable of total tumor eradication, which increases the probability of cancer recurrence, and can produce a powerful selective pressure which leads to diminished sensitivity to chemotherapeutics and radiation, and negatively affects prognosis [6,7]. To improve outcomes, thermal ablation is a promising alternative treatment modality, and has been introduced to clinical applications for combating a broad variety of malignant tumors, including liver, breast, cervix, bladder, brain, head, and neck tumors [8–11]. Selection of an appropriate means for heat

delivery to the tumor, however, presents an important challenge in thermal ablation. In these therapies, the energy source for inducing heat during thermal ablation procedures includes radiofrequencies (radiofrequency ablation, RFA), microwaves (microwave ablation, MWA), acoustic waves (high intensity focused ultrasound ablation (HIFU)), and laser ablation (photothermal ablation, PTA). The benefits of thermal ablation therapy over conventional methods include flexibility, low cost, and minimal invasiveness. However, such conventional hyperthermia generates a temperature gradient with a maximum on the hot spot that instantaneously decreases with distance from the external source (i.e., outside-in hyperthermia) (Figure 1). As a consequence, in order to reach underlying tumors, the activating energy source must sufficiently penetrate healthy tissues [12–14]. This non-selective heat destruction between tumors and the surrounding normal tissue can lead to serious side effects. These major disadvantages must be fully addressed in the development of an efficient hyperthermia method.

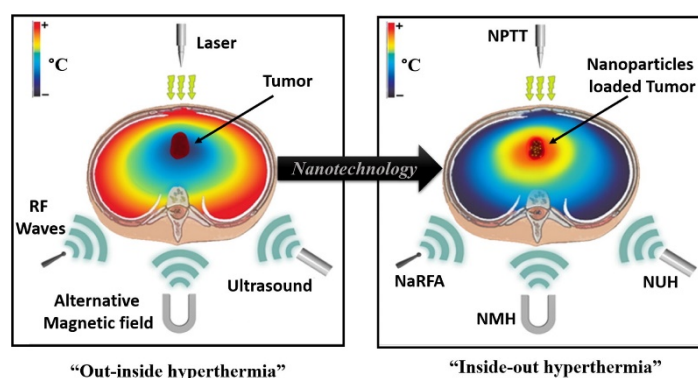


**Figure 1.** Thermal hyperthermia of a tumor using nanoparticles enclosed inside of it, absorbing the energy coming from different heat sources. NPTT: Nano-Photothermal Therapy; NMH: Nano-Magnetic Hyperthermia; NaRFA: Nano-Radio-Frequency Ablation; NUH: Nano-Ultrasound Hyperthermia. Reproduced from [13], with permission from Elsevier, Copyright 2016.

Over the past several decades, continuing efforts have been made towards attaining an optimal combination of nanomaterials and thermal therapy to overcome the relevant constraints of conventional thermal therapies. Among various nanomaterials investigated for thermal applications, gold nanoparticles (AuNPs) with localized surface plasmon resonance (LSPR) have been the most extensively investigated due to their high photothermal conversion efficiency, chemical/biological inertness, low cytotoxicity, ease of synthetic manipulation, and rapid surface functionalization for enhanced targeted delivery [15,16]. Plasmon resonance is a collective motion of a large number of electrons. When the frequency of an incident electromagnetic field matches the surface electrons of oscillating gold nanoparticles, the laser electric field strongly drives mobile electrons inside the nanocrystals, and the energy gained by mobile electrons turns into heat. Then the heat diffuses away from the nanocrystal and leads to an elevated temperature of the surrounding medium [17–19]. In nanoparticle-based hyperthermia, AuNPs with many mobile electrons can absorb energy originated from an external source, and then generate the primary source of heat and reverse the direction of heat loss (i.e., inside-out hyperthermia) to induce localized thermal destruction while minimizing adverse effects on surrounding normal tissues. Encouraged by the fact that several gold nanomaterials have recently translated into clinical evaluations (Table 1), significant effort has resulted in the recent proliferation of gold nanomaterials-mediated photothermal therapy (PTT) in the literature, including gold nanorods (AuNRs) [20–22], hollow gold nanospheres (HGNs) [21,23], gold nanocages (AuNCs) [24,25], gold nanobipyramids (AuBPs) [26,27], the assembly of gold nanoparticles [28–30], as well as multi-branched gold nanostructures, e.g., gold nanoflowers (AuNFs) [31–33], gold nanostars (AuNSs) [34,35], gold nanoechinus (AuNEs) [36,37],

and gold plasmonic blackbodies (AuPBs) [38]. However, effective translations of these modalities to clinical settings have not yet been achieved.

The clinical effectiveness of phototherapies is highly dependent on exposure time, total light dose, and light delivery type. Herein, we first focus on advanced designs of gold nanomaterials in laser-based photothermal therapy, followed by their adequate “therapeutic window”, in which the electron oscillation frequency of gold nanomaterials matches with incident light frequency and exhibits maximum penetration depth for deep tissue tumor ablation. Moreover, traditional “always-on” gold nanomaterials have been restricted in clinical translation due to their nonspecific response and side effects on normal tissues. Therefore, very recent advances in designing activatable (turn-on) AuNPs-mediated PTT are provided here. Finally, insights into the combinatory effect of AuNPs-mediated PTT and standard therapies are discussed, focusing on effective clinical applications and ongoing clinical trials, together with challenges facing the clinical translation of these AuNPs-mediated PTT.

**Table 1.** Clinical trials on gold nanomaterials.

| Product             | Pathology  | Type of AuNP                                     | Clinical Trial ID | Status/Date (First-Last Posted) | Application   | Reference |
|---------------------|--|--|-------------------|---------------------------------|---|-----------|
| NANOM FIM *         | Atherosclerotic lesions  | Silica-gold nanoparticle                         | NCT01270139       | Completed Jan 2011–June 2019    | Plasmonic photothermal therapy  | [39]      |
| NANOM PCI *         | Atherosclerosis  | Gold nanoparticles with silica-iron oxide shells | NCT01436123       | Terminated Sep 2011–May 2015    | Plasmonic photothermal and stem cell therapy  | [40]      |
| AuroLaseR *         | Head and neck cancer   | Silica-gold nanoshells coated with PEG           | NCT00848042       | Completed July 2016–Feb 2017    | Thermal ablation of solid tumors via NIR laser  | [41]      |
|                     | Primary and/or metastatic lung tumors                                |  | NCT01679470       | Sep 2012–Nov 2016               | Thermal ablation of solid tumors via NIR laser  |           |
|                     | Neoplastic prostate tissue   |  | NCT02680535       | Completed Feb 2016–Mar 2021     | Fusion imaging and biopsy in combination with nanoparticle directed focal therapy for ablation of tumor cells       | [42]      |
| NU-0129             | Gliosarcoma and recurrent glioblastoma                               | A spherical nucleic acid (SNA) gold nanoparticle | NCT03020017       | Completed Jan 2017–Oct 2020     | Safety evaluation of NU-0129  | [43]      |
| CNM-Au8             | Healthy volunteers   | Nanocrystal of gold                              | NCT02755870       | Completed Apr 2016–Jun 2019     | Safety evaluation, pharmacokinetics and tolerability of CNM-Au8   | [44]      |
| AuNPs               | Malignant or benign gastric lesions                                  | AuNPs with functionalized sensors                | NCT01420588       | Completed Aug 2011–May 2020     | Gastric lesions detection   | [45]      |
| AuNPs               | Healthy volunteers and patients with idiopathic and/or heritable PAH | AuNPs with functionalized sensors                | NCT02782026       | Completed May 2016–May 2021     | Detection of pulmonary arterial hypertension (PAH)  | [46]      |
| CYT-6091 (Aurimune) | Primary and metastatic cancer  | TNF-bound colloidal Gold                         | NCT00436410       | Completed Feb 2007–May 2012     | An evaluation of the tissue distribution and the selective tumor trafficking  | [47]      |
|                     | Advanced solid tumors  |  | NCT00356980       | Completed July 2006–Mar 2012    | Studying the side effects and best dose of TNF-bound colloidal gold in treating patients with advanced solid tumors | [48]      |

\* PTT based on AuNPs.

## 2. Gold Nanomaterials with Improved Photothermal Performance

It is well known that the heating performance of plasmonic nanoparticles depends on cellular uptake, internalization, accumulation, and photothermal conversion efficiency. Zhang et al. reported that the intravenous administration of AuNPs exhibited minimal toxicity compared with oral and intraperitoneal injections [49]. Their study suggested that the intravenous injection route could potentially constitute an appropriate route for delivering AuNPs [46]. However, a challenge associated with the delivery of nanoparticles through intravenous injection is that only a small fraction of the injected nanoagents (less than 10%) is able to reach the tumor, due to the rapid uptake and clearance of nanoparticles by reticuloendothelial system (RES) organs (e.g., liver, spleen, etc.) [50,51]. In addition, the assembly of plasmonic nanomaterials is likely to decrease its photothermal conversion efficiency because the contribution of scattering to extinction gradually increases as endocytosis progresses [52,53]. All of the above-mentioned factors indicate that a certain concentration of plasmonic nanoparticles is required to ensure sufficient nanoagents in the tumor site and guarantee the intended therapeutic effect.

Fortunately, based on high extinction coefficients, as well as excellent photothermal conversion efficiencies (PCE,  $\eta$ ), gold nanomaterial-mediated PTT both enables high heating generation and reduces the total nanoparticle administered dose. In the past two decades, gold nanorods and nanoshells have attracted great interest because the plasmon resonance can be “tuned” to any wavelength desired across a large region of the visible and infrared spectrum by adjusting the aspect ratio and the relative size of the inner and outer shell layer, respectively [54,55]. In 2003, the first gold nanoshell-mediated PTT report was presented by Hirsch et al., who successfully achieved localized, irreversible photothermal ablation of tumor tissue both *in vitro* and *in vivo* [56]. In addition, that study observed maximal depths of heating at depths beyond 1 cm with no observable damage to the intervening tissue. Shortly afterwards, anti-EGFR antibody-conjugated AuNRs, which were developed by El-Sayed’s group, demonstrated the selective and efficient photothermal killing of targeted tumor cells [57]. They also systematically evaluated the tunable absorption wavelength phenomenon and various aspect ratios of AuNRs. With their other advantages, including efficient large-scale synthesis, easy functionalization and colloidal stability, AuNRs have been demonstrated to be effective for the photothermal killing of cancer cells *in vitro* and *in vivo*. Furthermore, AuNRs with diameters smaller than 10 nm are dominated by absorption, which could minimize the impact of the scattering cross-section, which will improve the PCE [58,59]. Song et al. also developed a new plasmonic vesicle for photoacoustic (PA) imaging guided PTT based on ultras-small AuNRs (dimension:  $\approx 8 \times 2$  nm) [60]. They tested the photothermal effect of AuNR vesicles in comparison with AuNRs by acquiring the PA signal and evaluating tumor ablation upon 808 nm laser irradiation. Compared with AuNRs, the PCE of the vesicles can reach 51%, which is approximately two-fold higher than AuNRs (23%). In addition to nanorods and nanoshells, the extant literature has explored other nanocrystal shapes on the PCE (Table 2). For instance, the finite-difference time-domain (FDTD) simulation was utilized by Yang et al. to report shape-dependent electric field distribution for gold nanospheres, gold nanorods, and gold nanostars [61]. They demonstrated that the strongest electric field at the tips of gold nanostars can induce the largest number of hot spots by the surface plasmon resonance effect, and the gold nanostars exhibited higher photothermal conversion efficiency (46.18%) than gold nanospheres (21.6%) and gold nanorods (20.4%).

Recently, to improve the photothermal conversion ability of gold nanomaterials, core-shell hybrid nanomaterials have become increasingly common [62–64]. These AuNP-plasmonic hybrid structures can improve plasmon-based photothermal conversion through two effects. The first effect is the shift in the characteristic absorption peak arising from the change in the refractive index of the particle environment. Repenko et al. successfully introduced gold-core melanin-shell nanoparticles with different geometries from spheres to nanostars and nanorods [63]. They found that all melanin polymer coated particles showed an increased photoacoustic signal compared to their respective pristine gold core particle.

These results indicate that the melanin shell, which is a stable photothermal coupling agent, provides additional electron oscillation and enhances photothermal conversion efficiency. In addition to a polymer shell, inorganic materials, such as semiconductors, silica and carbon materials, have been widely utilized to change plasmonic properties due to the increase in the refractive index of the local dielectric environment of the Au core. For example, AgS<sub>2</sub> with a small band gap (0.9–1.1 eV) enhances overall NIR light absorption and improves photothermal conversion efficiency owing to the presence of an additional light absorption channel [59,65].

When gold nanomaterials were internalized by cancer cells and confined in endosomes/lysosomes, an increase in diameter would be expected to correspond with an increase in the contribution of scattering to extinction (and thereby a decrease in the absorption component and resultant PCE). Interesting, Lindley et al. investigated the influence of surface protrusions on the PCE of hollow gold nanospheres. They tested the photothermal conversion efficiency calculations for both smooth and bumpy HGNs [23]. Within this test, all of the HGNs exhibited excellent heat generation, with up to 99% photothermal conversion efficiency. However, an interesting phenomenon was observed, in that bHGNs were capable of nearly equivalent heat generation as their smaller smooth counterparts, which may be ascribed to the efficient reabsorption of scattered light. Indeed, this is not surprising considering the findings of Zhou et al., in which Au plasmonic blackbody (AuPB) with a high density of randomly-oriented branches afforded broadband absorption spanning the entire UV-Vis-NIR range (400–1350 nm) and polarization [38].

**Table 2.** Photothermal conversion efficiency of gold nanomaterials.

| Type   | Irradiation Wavelength (nm) | PCE ( $\eta$ ) (%) | Ref.    |
|--|-----------------------------|--------------------|---------|
| <b>Structure</b>   |                             |                    |         |
| Gold nanoshells  | 800 nm                      | 13%, 39%           | [66,67] |
| Gold nanorods  | 800 nm                      | 21%                | [66]    |
| Gold Nanomatryoshkas   | 810 nm                      | 63%                | [67]    |
| Gold hexapod   | 808 nm                      | 29.6%              | [68]    |
| Gold nanocage  | 808 nm                      | 63.6%              | [68]    |
| Gold nanostars   | 800 nm                      | 38 $\pm$ 3%        | [69]    |
| Gold nanocup   | 808 nm                      | 38.5%              | [70]    |
| Gold nanospikes  | 808 nm                      | 50.3%              | [71]    |
| Gold bellflower  | 808 nm                      | 74%                | [72]    |
| <b>Enhancing plasmonic coupling</b>                              |                             |                    |         |
| Gold nanorod covered by layered double hydroxides (GNR@LDH)      | 808 nm                      | 60%                | [62]    |
| Gold nanoparticle coated carbon nanotube ring (CNTR@AuNS)        | 808 nm                      | 76%                | [64]    |
| Gold-nanobranched coated betulinic acid liposomes (GNBS-BA-Lips) | 808 nm                      | 55.7%              | [73]    |
| <b>Enhancing scattering reabsorbance</b>                         |                             |                    |         |
| Bumpy hollow gold nanospheres (bHGNs)                            | 808 nm                      | 99%                | [23]    |
| Biodegradable gold nanovesicles (BGVs)                           | 808 nm                      | 37%                | [28]    |
| Gold plasmonic blackbody (AuPB)                                  | 808 nm                      | 88.6%              | [38]    |
|  | 1064 nm                     | 80.8%              |         |

### 3. Development of Second Near-Infrared Photothermal Agents

For topical PTT treatments, light irradiation of deep-seated tissue can be achieved by balloon catheters. It is well established that the reachable depth (region) of PTT relies on the penetration depth of the excitation light. To further increase tissue penetration depth, second NIR (NIR-II, 1000–1700 nm) light has emerged (Figure 2A). Thus far, although various types of AuNPs have been reported, the NIR-II window-related properties of plasmonic AuNPs have rarely been investigated, while most types have LSPR peaks in the NIR-I window (700–950 nm). Considering the practical feasibility of gold nanomaterials,



AuNRs is one of the potential candidates for tuning the LSPR into the NIR-II regions. Unfortunately, AuNR, with an SPR band extended to 1000 nm (Figure 2B), possesses significant limitations for biomedical applications because the length of an AuNR is usually extended to 300–600 nm, which is larger than the traditional particle size of 10–200 nm and is difficult to internalize by cells [74,75]. To circumvent this problem, Tsai et al. designed a rod-in-shell (rattle-like) AuNRs with a size smaller than 100 nm and with two distinct SPR peaks at approximately 1100 and 1280 nm [17]. They demonstrated that tuning the gap distance between the AuNR (core) and the nanoshell could shift absorption bands into the NIR-II region. Moreover, the photothermal ablation of solid tumors in both 808 nm (NIR-I window) and 1064 nm (NIR-II window) showed excellent efficacy (Figure 2C). Recently, anisotropic AuNPs (i.e., flowers, urchins, or stars) with sharp and elongated branches have aroused great interest in biologically-related applications of NIR-II. The gold nanomaterial described in the section above, i.e., AuPB, exhibits superior photothermal transduction (approximately 98.5% of the total extinction comes from absorption), as a consequence of the small size and strong coupling of the hyperbranched nanostructure. Similarly, gold nanoraspberry and gold nanoechinus were developed by Lalatonne’s group and Hwang’s group, respectively [36,76]. A major shortcoming of multibranched gold nanoparticles-mediated PTT is that they tend to strongly scatter NIR light, causing a significant reduction in absorption. Bi et al. investigated the core size, tip numbers, length, and widths on PCE. Compared to the traditionally hyperbranched AuNPs (popcorn-like), spiky AuNPs with long tips and a small core not only shift the maximum SPR peak to the NIR-II window, but also exhibit high Cabs/Csca, thus causing excellent photothermal conversion efficiency (78.8%) [77]. This research provided important information for the design of gold nanomaterials with various architectural structures. Based on these principles, the first gold multipods were developed by Li and coworkers [78]. They demonstrated an Fe template-directed method for generating Au multipods with small core and long arm length. However, the first application of gold multipods (Au<sub>3</sub>Cu TPNCs) in NIR-II PTT was proposed by Wang et al. in 2018 [79]. Au<sub>3</sub>Cu exhibited a greater temperature increment under a 1064 nm irradiation than that at 808 nm, and the PCT values of Au<sub>3</sub>Cu TPNCs were calculated as 39.45% at 808 nm and as 75.27% at 1064 nm. Au<sub>3</sub>Cu TPNCs also showed an excellent ability for NIR-II PA imaging, and could serve as multimodality imaging-guided NIR-II agents.

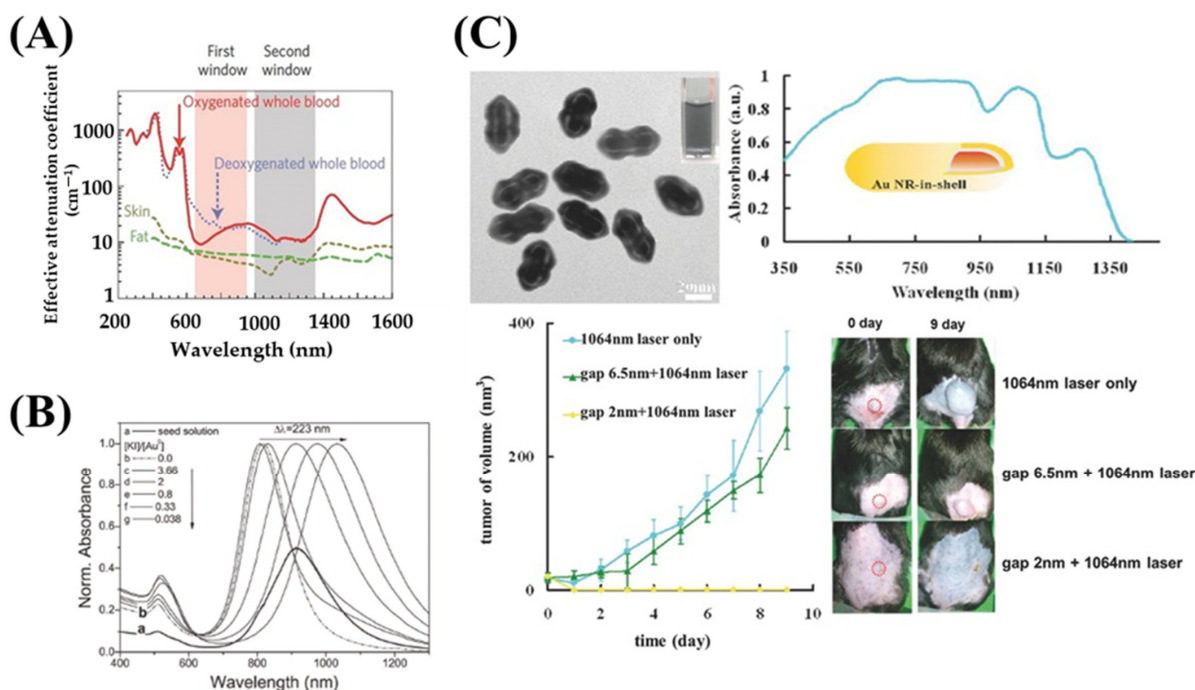
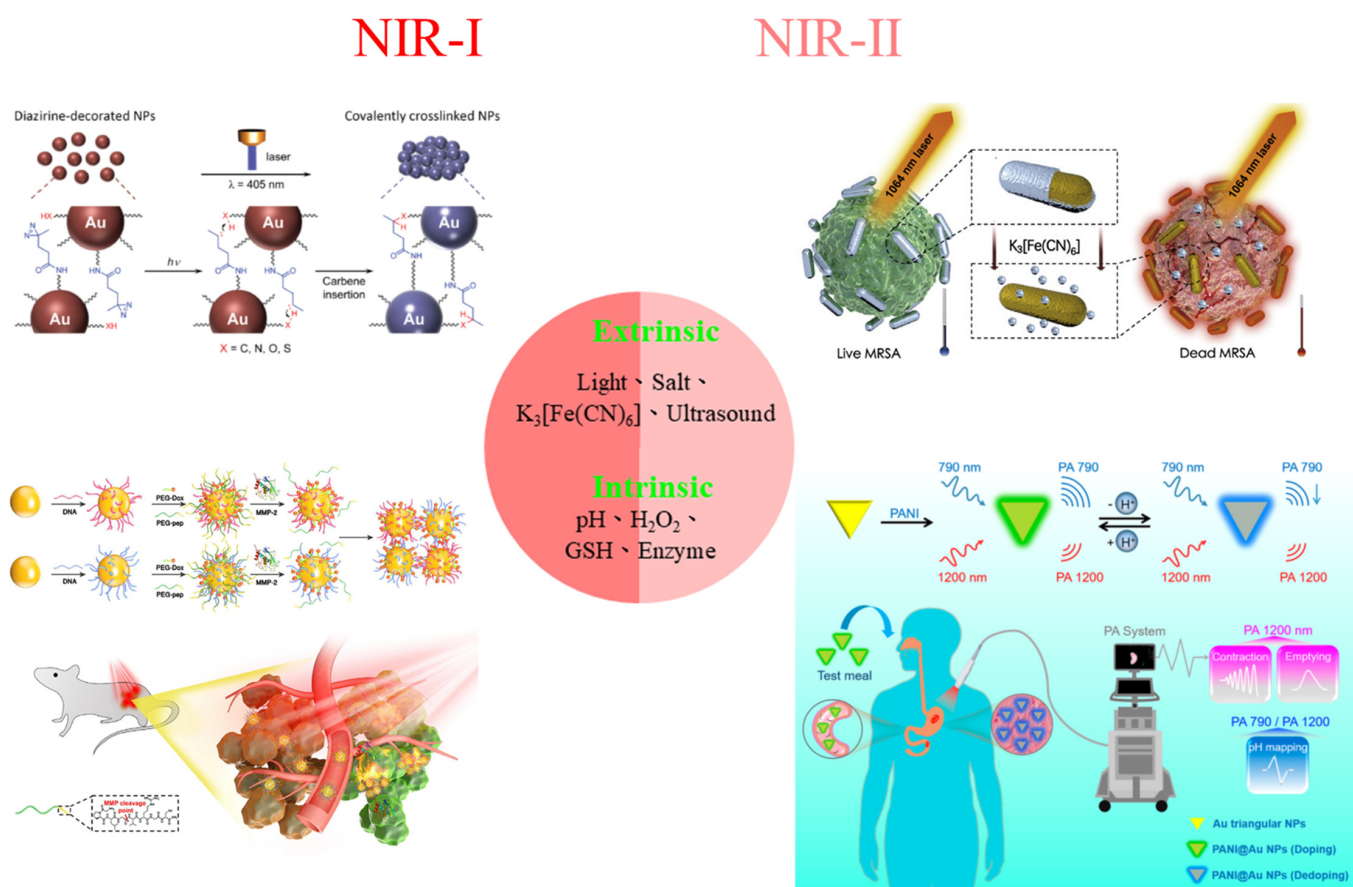


Figure 2. (A) Plot of the wavelength-dependent effective attenuation coefficient showing optical windows

in biological tissues. (B) Representative examples of NIR-II-window-responsive plasmonic nanomaterials: AuNRs (C) Transmission electron microscopy (TEM) image and UV-visible-NIR spectrum of Au rod-in-shell nanostructures, and photographs showing the photothermal therapeutic effect. The red dotted circles indicate the location of the tumors. Figures from: (A) Adapted with permission [80]. John Wiley and Sons, Copyright 2017; (B) Adapted with permission [81]. John Wiley and Sons, Copyright 2008; (C) Adapted with permission [20]. American Chemical Society, Copyright 2013.

#### 4. Development of Activatable NIR Photothermal Agents

With the development of AuNPs mediated PTT in recent years, increasing effort has been devoted to solving two major defects. As mentioned above, many different strategies have become available to shift the working window into the NIR-II region, which has attracted substantial attention due to the higher maximum permissible exposure (e.g., 1064 nm,  $1.0 \text{ W}\cdot\text{cm}^{-2}$ ), lower biology background, and deeper penetration depth versus the NIR-I region. On the other hand, the therapeutic specificity of AuNPs mediated PTT depends on the specific delivery of gold nanomaterials and NIR laser irradiation to tumors, and most photothermal agents with “always on” mode suffer from inherent non-specificity and undesirable treatment-related side effects. In contrast, the design of activatable or smart photothermal agents offers an innovative approach to interact with targets of interest, allowing for the precise and effective suppression of cancer without side effects. These stimulus-responsive agents use the unique characteristics of the tumor microenvironment, including mild acidic nature, disordered redox potentials and hypoxia, as well as the overexpressed specific enzymes, to achieve “off” to “on” switching tumor-specific detection and therapy (Figure 3). For instance, Kim et al. reported a pH-responsive AuNPs that can agglomerate at the tumorous site and elicit a significant absorption wavelength shift into the NIR optical window to spare normal cells and minimize unwanted damage [82]. Other gold-based pH-responsive photothermal agents are reported by both Liu’s and Wong’s groups [83,84]. These nanoagents could intelligently respond to the tumor acidic microenvironment, which converts the surface charge. As a result, the nanoparticles aggregate rapidly via electrostatic attraction, lighting up the NIR absorbance and increasing the PCT of low-to-high energy excitation. Furthermore, accumulated evidence indicates that the amounts of matrix metalloproteinases (MMPs) protein, especially MMP-2 and MMP-9, are significantly increased in patients with advanced cancers [85–87]. Therefore, Yang et al. designed a nanoplatfrom based on matrix metalloproteinase (MMP)-responsive gold nanoparticles (AuNPs) for tumor-targeted photoacoustic (PA) imaging-guided synergistic chemo-photothermal therapy [88]. In general, the PEG is conjugated onto AuNPs through an MMP-sensitive peptide to coat and protect intact AuNPs in blood circulation. The PEG is then locally released in tumor triggered by over-expressed MMPs, and then the complementary DNA strands are exposed on the nanoparticle surface. Driven by DNA hybridization, the nanoparticles rapidly aggregated and induced the redshift of their absorption into the NIR region. The assembly strategy exhibited a stronger and broader NIR absorption band, ranging from 650 to 850 nm), which facilitated AuNPs to enhance imaging signals and the photothermal efficacy of PA imaging and PTT under irradiation of an 808 nm laser [88]. Similarly, Ruan et al. prepared a legumain-induced assembly of gold nanoparticles (AuNP-DOX-A&C) to improve their accumulation in glioblastoma (GBM) [89]. AuNP-DOX-A&C could click-cycload in the activation of legumain, resulting in the in situ formation of AuNP aggregates. Under 690 nm irradiation, the nanoplatfrom showed excellent PA signal enhancement (1.9-fold) in the tumor site compared to the control group.



**Figure 3.** Activatable gold nanomaterials for PA imaging and PTT. Reprinted with permission from ref [88,90–92].

Despite the very recent advances in designing “turn-on” phototherapy agents, activatable AuNPs based photothermal agents for the NIR-II region remain rare, some of which are summarized and compared in Table 3. To date, some organic photothermal agents have been synthesized, which could switch photothermal therapy and photoacoustic imaging from “off” to “on” upon stimulation [93,94]. However, these photosensitizers are neither simple to prepare nor resistant to photobleaching. More recently, Liu et al. reported a smart hydrogen peroxide ( $\text{H}_2\text{O}_2$ )-activable silver-coated gold nanostars ( $\text{Au}@\text{Ag}$ ) for NIR-II PTT and PA imaging of tumors and lymph node metastasis [95]. In the presence of  $\text{H}_2\text{O}_2$ , the Ag shell of Au/Ag nanostars was effectively etched, and free  $\text{Ag}^+$  was released to eliminate cancer. Meanwhile, the Au/Ag nanostars residue enhanced NIR-II PA performance and enabled monitoring of signal molecule dynamics, the real-time PA imaging of tumors, and lymph node metastasis. In the same year, and based on a similar theory, Ye and coworkers designed a novel  $\text{H}_2\text{O}_2$ -responsive theranostic nanoplatform comprising Ag shell coated Pd-tipped gold nanorods ( $\text{Au-Pd}@\text{Ag}$  NR) for both NIR-I and NIR-II PA imaging. The ratiometric PA imaging at 1260 and 700 nm ( $\text{PA}_{1260}/\text{PA}_{700}$ ) accurately quantifies  $\text{H}_2\text{O}_2$  in a mice model of bacterial infection and in a rabbit model of osteoarthritis [96]. This report proposed the concept of synergistic anticancer activity which showed tremendous potential for activatable NIR-II theranostic application.



**Table 3.** Summary of recent reports on activatable gold nanomaterials for PA imaging/PTT.

| Activable NIR Photothermal Agents        | Physiological Parameters              | Laser Irradiation | Exp. Subject             | Ref.  |
|--|---------------------------------------|-------------------|--------------------------|-------|
| PEG/RGD/NLS/AuNSs                        | Intracellular assembly                | 808 nm            | in vitro                 | [53]  |
| c(RGDyk)-MHDA/LSC@AuNP                   | pH                                    | 680–950 nm        | in vitro/in vivo (i.v.)  | [84]  |
| PEG-pep-Dox-AuNPs                        | MMP                                   | 808 nm            | in vitro/in vivo (i.v.)  | [88]  |
| dAuNPs                                   | Light                                 | 808 nm            | in vitro/in vivo (i.v.)  | [90]  |
| Au/Ag NRs                                | K <sub>3</sub> [Fe(CN) <sub>6</sub> ] | 1064 nm           | in vitro/in vivo (local) | [91]  |
| Polyaniline and Au triangular nanoplates | pH                                    | 790 nm/1200 nm    | in vivo (oral)           | [92]  |
| Au-Pd@Ag                                 | H <sub>2</sub> O <sub>2</sub>         | 700 nm/1260 nm    | in vitro/in vivo (local) | [96]  |
| AuNPs                                    | Salt                                  | 808 nm            | in vitro/in vivo (i.t.)  | [97]  |
| Au-RRVR                                  | pH /furin                             | 808 nm            | in vitro/in vivo (i.v.)  | [98]  |
| AuNR@PEG/PolyRu Ves                      | Light                                 | 1240 nm           | in vitro/in vivo (i.v.)  | [99]  |
| JNP Ve                                   | Ultrasound/GSH                        | 808 nm/1260 nm    | in vitro/in vivo (i.v.)  | [100] |

## 5. Future Challenges

Owing to its extraordinary physicochemical properties, AuNP is one of the most attractive materials in the field of developing cancer theragnosis. Indeed, a dramatically increasing number of clinical trials are being performed globally. It is considered that AuNPs-mediated PTT could become a viable alternative treatment to replace traditional methods in the management of cancer. Before such treatments can be translated to clinical settings, however, several challenges need to be overcome. First, in spite of the existence of various of gold nanomaterials, certain factors need to be addressed concerning synthesis. Synthesis methods with control that ensures reproducibility batch by batch, with sufficient yield of the morphology of interest, cost efficiency, well-defined properties, and potential scale-up are currently still lacking. Second, in order to synthesize gold nanoparticles with hierarchical architectures for NIR PTT, environmentally- and biologically-hazardous reagents, such as cetyltrimethylammonium bromide, Ag, Cu and organic solvent, are used in most documented methods. In particular, almost all NIR-II window-responsive gold nanomaterials are bimetallic alloys, which might induce toxicity during in vivo applications. For activatable NIR PTT gold nanomaterials, even though some researchers have attempted to solve this issue in the NIR-I window region, tumor microenvironment- induced assembly would enhance scattering and reduce the absorption of these materials, implying its low photoabsorption ability and ineffective photothermal conversion feature. Moreover, these challenges would be markedly worse in activatable NIR-II nanoagents. Furthermore, biocompatibility and biodegradation has been demonstrated as the key avenue regarding the issue for clinical application. As well as the synthetic biomineral-based nanocarriers, including calcium phosphate (Ca), magnesium phosphate (Mg), calcium carbonate (Ca), and iron oxide (Fe), etc., gold nanomaterials have been reported to exhibit high biocompatibility in vitro and in vivo. However, the degradation behavior and excretion pathway necessitate further evaluation. In 2020, Carn et al. reported a biodegradation phenomenon of 4 nm AuNPs. This degradation is mediated by NADPH oxidase that produces highly oxidizing reactive oxygen and generates biomineralized gold nanostructures [101]. This is consistent with the observation in our previous study [31]. Furthermore, some researchers engineered stimuli-responsive degradation of gold nanostructures to decrease the retention of gold through the effective clearance by renal clearance [28,30,102]. However, further understanding on the detailed biodegradation mechanisms, metabolic pathway, and toxicity assessment of gold nanomaterials are still progressing.

Finally, despite the above-mentioned strategies to improve penetration depth for radiation, eradicating solid tumors completely by AuNPs mediated PTT alone can still be difficult. Therefore, the combination of PTT with other conventional treatment strategies could result in supra-synergistic effects in cancer therapy. A common pattern is the combination of chemotherapy and PTT. Chemotherapy can address the limitation of light

penetration in phototherapy, whereas a mild photothermal heating reduces the extracellular matrix barrier and increases blood flow. In addition, hyperthermia increases cell membrane permeability and enhances the intracellular delivery of therapeutic agents, which circumvents traditional drug resistance mechanisms. Owing to its high atomic number (Z), AuNP enhances the local absorbed dose of X-rays and may improve the efficiency of radiotherapy. In fact, numerous clinical experiments conducted on breast, cervix, bladder, brain, head, and neck tumors have demonstrated that the addition of hyperthermia to radiotherapy significantly improves tumor control and patient survival rates [13,103,104]. As a result, AuNPs mediated PTT possesses great potential for clinical translation. The induction of a systemic anticancer immune response through localized photoablation is based on the fact that cancer cells die because of heat to release damage-associated molecular patterns, which are further captured by antigens present in the body to mediate the immune response. Accordingly, researchers have initiated efforts to exploit immunogenic cell death (ICD) arising from PTT to augment the efficacy of immunotherapy. For instance, Zhang et al. firstly demonstrated that temperature-dependent necroptosis is an important mechanism of inducing melanoma cell death in GNR-mediated PTT [105]. In the same year, Sweeney et al. presented a novel concept: a thermal “window” of ICD [106]. They demonstrated that nanoparticles mediated PTT triggered ICD markers highly expressed within an optimal temperature (thermal dose) window (63.3–66.4 °C) as compared with higher (83.0–83.5 °C) and lower (50.7–52.7 °C) temperatures. Subsequently, a further immunostimulatory environment is developed by the PTT. Therefore, the combination of AuNPs mediated PTT with immunotherapy has the potential to effectively eradicate the target tumor, and could also trigger immunological memory to prevent tumor recurrence.

## 6. Conclusions

Over the two past decades, the field of AuNP-based PTT has experienced tremendous growth, as evidenced by the dramatic increase in the number of publications and clinical trials. Indeed, AuNP-based PTT possesses multiple major benefits in comparison to conventional thermal ablation, as the former treatment modality enables utilization of inside-out hyperthermia to induce localized thermal destruction while simultaneously minimizing deleterious effects on surrounding normal tissues. Overall, the therapeutic effect of excitation by lower particle dosage and the longer wavelength of light can effectively decrease side effects and achieve the specific treatment. Based on the findings to date, recent advancements have focused on exploiting the synthetic versatility of AuNPs to develop higher PCE, deeper penetration depth and smarter gold nanomaterials, and on expanding the clinical utility of AuNP photothermal agents. These findings will assist with the design and development of AuNP photothermal agents with ideal features for clinical implementation. However, several issues may still need to be addressed, such as those involving safety and in vivo efficacy, which may be limiting the translation of these innovative strategies. AuNPs mediated PTT is demonstrated to constitute a promising approach in laboratory and preclinical research. It is reasonably expected that the use of AuNPs for PTT will gradually translate to clinical settings. Moreover, in addition to using this technology alone, AuNPs mediated PTT has shown significant synergistic therapeutic effects when combined with other conventional therapies, such as radiotherapy, chemotherapy, and immunotherapy. Indeed, the combination of different strategies has also been shown to reduce the side effects of a single therapy. For instance, PTT/chemo and PTT/radio co-therapy is renowned for its synergistic effects. It is worth noting, however, that current knowledge of the use of immune response induced by PTT is still in its nascent stage. In order to exploit all of the opportunities offered by PTT/immunotherapy combinational therapy, as well as to identify areas that may need improvement, more comprehensive understanding and systematic investigations are needed.

**Author Contributions:** Resources, J.-F.C. and L.-W.L.; Writing—original draft preparation, Y.-C.C.; Writing—review and editing, H.-L.L. and L.-W.L.; Supervision, J.-F.C. and L.-W.L.; funding acquisition, L.-W.L. All authors have read and agreed to the published version of the manuscript.

**Funding:** This publication was supported by the Ministry of Science and Technology of Taiwan under award No. MOST 105-2113-M-400-007-MY3 and MOST 110-2112-M-400-001. This publication was supported by the National Health Research Institutes of Taiwan under award No. 06A1-PP04-014.

**Institutional Review Board Statement:** Not applicable.

**Informed Consent Statement:** Not applicable.

**Acknowledgments:** We would also like to acknowledge the work Maharajan Sivasubramanian and Jake Carpenter in providing editorial support.

**Conflicts of Interest:** The authors declare that they have no conflicts of interest.

## References

1. Sung, H.; Ferlay, J.; Siegel, R.L.; Laversanne, M.; Soerjomataram, I.; Jemal, A.; Bray, F. Global Cancer Statistics 2020: GLOBOCAN Estimates of Incidence and Mortality Worldwide for 36 Cancers in 185 Countries. *CA Cancer J. Clin.* **2021**, *71*, 209–249. [[CrossRef](#)] [[PubMed](#)]
2. Ferlay, J.; Colombet, M.; Soerjomataram, I.; Parkin, D.M.; Piñeros, M.; Znaor, A.; Bray, F. Cancer Statistics for the year 2020: An overview. *Int. J. Cancer* **2021**, *149*, 778–789. [[CrossRef](#)] [[PubMed](#)]
3. Cortez, A.J.; Tudrej, P.; Kujawa, K.A.; Lisowska, K.M. Advances in Ovarian Cancer Therapy. *Cancer Chemother. Pharmacol.* **2018**, *81*, 17–38. [[CrossRef](#)] [[PubMed](#)]
4. Grégoire, V.; Guckenberger, M.; Haustermans, K.; Lagendijk, J.J.W.; Ménard, C.; Pötter, R.; Slotman, B.J.; Tanderup, K.; Thorwarth, D.; van Herk, M.; et al. Image Guidance in Radiation Therapy for Better Cure of Cancer. *Mol. Oncol.* **2020**, *14*, 1470–1491. [[CrossRef](#)] [[PubMed](#)]
5. Hughes, J.R.; Parsons, J.L. FLASH radiotherapy: Current Knowledge and Future Insights Using Proton-Beam Therapy. *Int. J. Mol. Sci.* **2020**, *21*, 6492. [[CrossRef](#)] [[PubMed](#)]
6. Bukowski, K.; Kciuk, M.; Kontek, R. Mechanisms of Multidrug Resistance in Cancer Chemotherapy. *Int. J. Mol. Sci.* **2020**, *21*, 3233. [[CrossRef](#)] [[PubMed](#)]
7. Krisnawan, V.E.; Stanley, J.A.; Schwar, J.K.; DeNardo, D.G. Tumor Microenvironment as a Regulator of Radiation Therapy: New Insights into Stromal-Mediated Radioresistance. *Cancers* **2020**, *12*, 2916. [[CrossRef](#)]
8. Izadifar, Z.; Izadifar, Z.; Chapman, D.; Babyn, P. An Introduction to High Intensity Focused Ultrasound: Systematic Review on Principles, Devices, and Clinical Applications. *J. Clin. Med.* **2020**, *9*, 460. [[CrossRef](#)]
9. Elhelf, I.A.S.; Albahar, H.; Shah, U.; Oto, A.; Cressman, E.; Almekkawy, M. High Intensity Focused Ultrasound: The Fundamentals, Clinical Applications and Research Trends. *Diagn. Interv. Imaging* **2018**, *99*, 349–359. [[CrossRef](#)]
10. An, C.; Li, X.; Zhang, M.; Yang, J.; Cheng, Z.; Yu, X.; Han, Z.; Liu, F.; Dong, L.; Yu, J.; et al. 3D Visualization Ablation Planning System Assisted Microwave Ablation for Hepatocellular Carcinoma (Diameter >3): A Precise Clinical Application. *BMC Cancer* **2020**, *20*, 44. [[CrossRef](#)]
11. Zhu, F.; Rhim, H. Thermal Ablation for Hepatocellular Carcinoma: What's New in 2019. *Chin. Clin. Oncol.* **2019**, *8*, 58. [[CrossRef](#)]
12. Ashikbayeva, Z.; Tosi, D.; Balmassov, D.; Schena, E.; Saccomandi, P.; Inglezakis, V. Application of Nanoparticles and Nanomaterials in Thermal Ablation Therapy of Cancer. *Nanomaterials* **2019**, *9*, 1195. [[CrossRef](#)]
13. Beik, J.; Abed, Z.; Ghoreishi, F.S.; Hosseini-Nami, S.; Mehrzadi, S.; Shakeri-Zadeh, A.; Kamrava, S.K. Nanotechnology in Hyperthermia Cancer Therapy: From Fundamental Principles to Advanced Applications. *J. Control. Release* **2016**, *235*, 205–221. [[CrossRef](#)]
14. Day, E.S.; Morton, J.G.; West, J.L. Nanoparticles for Thermal Cancer Therapy. *J. Biomech. Eng.* **2009**, *131*, 074001. [[CrossRef](#)]
15. Bansal, S.A.; Kumar, V.; Karimi, J.; Singh, A.P.; Kumar, S. Role of Gold Nanoparticles in Advanced Biomedical Applications. *Nanoscale Adv.* **2020**, *2*, 3764–3787. [[CrossRef](#)]
16. Elahi, N.; Kamali, M.; Baghersad, M.H. Recent Biomedical Applications of Gold Nanoparticles: A review. *Talanta* **2018**, *184*, 537–556. [[CrossRef](#)]
17. Govorov, A.O.; Richardson, H.H. Generating heat with metal nanoparticles. *NanoToday* **2007**, *2*, 30–38. [[CrossRef](#)]
18. Linic, S.; Aslam, U.; Boerigter, C.; Morabito, M. Photochemical transformations on plasmonic metal nanoparticles. *Nat. Mater.* **2015**, *14*, 567–576. [[CrossRef](#)]
19. Ji, M.; Liu, H.; Cheng, M.; Huang, L.; Yang, G.; Bao, F.; Huang, G.; Huang, Y.; Hu, Y.; Cong, G.; et al. Plasmonic metal nanoparticle loading to enhance the photothermal conversion of carbon fibers. *J. Phys. Chem. C* **2022**, *126*, 2454–2462. [[CrossRef](#)]
20. Tsai, M.F.; Chang, S.H.G.; Cheng, F.Y.; Shanmugam, V.; Cheng, Y.S.; Su, C.H.; Yeh, C.S. Au Nanorod Design as Light-Absorber in the First and Second Biological Near-Infrared Windows for in Vivo Photothermal Therapy. *ACS Nano* **2013**, *7*, 5330–5342. [[CrossRef](#)]
21. Cai, K.; Zhang, W.; Zhang, J.; Li, H.; Han, H.; Zhai, T. Design of Gold Hollow Nanorods with Controllable Aspect Ratio for Multimodal Imaging and Combined Chemo-Photothermal Therapy in the Second Near-Infrared Window. *ACS Appl. Mater. Interfaces* **2018**, *10*, 36703–36710. [[CrossRef](#)] [[PubMed](#)]
22. Du, C.; Wang, A.; Fei, J.; Zhao, J.; Li, J. Polypyrrole-Stabilized Gold Nanorods with Enhanced Photothermal Effect towards Two-Photon Photothermal Therapy. *J. Mater. Chem. B* **2015**, *3*, 4539–4545. [[CrossRef](#)] [[PubMed](#)]

23. Lindley, S.A.; Zhang, J.Z. Bumpy Hollow Gold Nanospheres for Theranostic Applications: Effect of Surface Morphology on Photothermal Conversion Efficiency. *ACS Appl. Mater. Interfaces* **2019**, *2*, 1072–1081. [[CrossRef](#)]
24. Skrabalak, S.E.; Chen, J.; Sun, Y.; Lu, X.; Au, L.; Cobley, C.M.; Xia, Y. Gold Nanocages: Synthesis, Properties, and Applications. *Acc. Chem. Res.* **2008**, *41*, 1587–1595. [[CrossRef](#)]
25. Xu, Q.; Wan, J.; Bie, N.; Song, X.; Yang, X.; Yong, T.; Zhao, Y.; Yang, X.; Gan, L. A Biomimetic Gold Nanocages-Based Nanoplatform for Efficient Tumor Ablation and Reduced Inflammation. *Theranostics* **2018**, *8*, 5362–5378. [[CrossRef](#)]
26. Xu, Y.; Wang, X.; Cheng, L.; Liu, Z.; Zhang, Q. High-Yield Synthesis of Gold Bipyramids for In Vivo CT Imaging and Photothermal Cancer Therapy with Enhanced Thermal Stability. *Chem. Eng. Sci.* **2019**, *378*, 122025. [[CrossRef](#)]
27. Campu, A.; Focsan, M.; Lerouge, F.; Borlan, R.; Tie, L.; Rugina, D.; Astilean, S. ICG-Loaded Gold Nano-Bipyramids with NIR Activatable Dual PTT-PDT Therapeutic Potential in Melanoma Cells. *Colloids Surf. B* **2020**, *194*, 111213. [[CrossRef](#)]
28. Huang, P.; Lin, J.; Li, W.; Rong, P.; Wang, Z.; Wang, S.; Wang, X.; Sun, X.; Aronova, M.; Niu, G.; et al. Biodegradable Gold Nanovesicles with an Ultrastrong Plasmonic Coupling Effect for Photoacoustic Imaging and Photothermal Therapy. *Angew. Chem. Int. Ed. Engl.* **2013**, *52*, 13958–13964. [[CrossRef](#)]
29. Chung, U.S.; Kim, J.H.; Kim, B.; Kim, E.; Jang, W.D.; Koh, W.G. Dendrimer Porphyrin-Coated Gold Nanoshells for the Synergistic Combination of Photodynamic and Photothermal Therapy. *Chem. Commun.* **2016**, *52*, 1258–1261. [[CrossRef](#)]
30. Tam, J.M.; Tam, J.O.; Murthy, A.; Ingram, D.R.; Ma, L.L.; Travis, K.; Johnston, K.P.; Sokolov, K.V. Controlled Assembly of Biodegradable Plasmonic Nanoclusters for Near-Infrared Imaging and Therapeutic Applications. *ACS Nano* **2010**, *4*, 2178–2184. [[CrossRef](#)]
31. Chuang, Y.C.; Hsia, Y.; Chu, C.H.; Lin, L.J.; Sivasubramanian, M.; Lo, L.W. Precision Control of the Large-Scale Green Synthesis of Biodegradable Gold Nanodandelions as Potential Radiotheranostics. *Biomater. Sci.* **2019**, *7*, 4720–4729. [[CrossRef](#)]
32. Jiang, T.; Yin, N.; Liu, L.; Song, J.; Huang, Q.; Zhu, L.; Xu, X. A Au Nanoflower@SiO<sub>2</sub>@CdTe/CdS/ZnS Quantum Dot Multifunctional Nanoprobe for Photothermal Treatment and Cellular Imaging. *RSC Adv.* **2014**, *4*, 23630–23636. [[CrossRef](#)]
33. Lu, W.; Singh, A.K.; Khan, S.A.; Senapati, D.; Yu, H.; Ray, P.C. Gold Nano-Popcorn-based Targeted Diagnosis, Nanotherapy Treatment, and In Situ Monitoring of Photothermal Therapy Response of Prostate Cancer Cells Using Surface-Enhanced Raman Spectroscopy. *J. Am. Chem. Soc.* **2010**, *132*, 18103–18114. [[CrossRef](#)]
34. Liu, Y.; Maccarini, P.; Palmer, G.M.; Etienne, W.; Zhao, Y.; Lee, C.T.; Ma, X.; Inman, B.A.; Vo-Dinh, T. Synergistic Immuno Photothermal Nanotherapy (SYMPHONY) for the Treatment of Unresectable and Metastatic Cancers. *Sci. Rep.* **2017**, *7*, 8606. [[CrossRef](#)]
35. Wang, S.; Huang, P.; Nie, L.; Xing, R.; Liu, D.; Wang, Z.; Lin, J.; Chen, S.; Niu, G.; Lu, G.; et al. Single Continuous Wave Laser Induced Photodynamic/Plasmonic Photothermal Therapy Using Photosensitizer-Functionalized Gold Nanostars. *Adv. Mater.* **2013**, *25*, 3055–3061. [[CrossRef](#)]
36. Vijayaraghavan, P.; Liu, C.H.; Vankayala, R.; Chiang, C.S.; Hwang, K.C. Designing Multi-Branched Gold Nanoechinus for NIR Light Activated Dual Modal Photodynamic and Photothermal Therapy in the Second Biological Window. *Adv. Mater.* **2014**, *26*, 6689–6695. [[CrossRef](#)]
37. Zhang, B.; Wang, J.; Sun, J.; Wang, Y.; Chou, T.; Zhang, Q.; Shah, H.R.; Ren, L.; Wang, H. Self-Reporting Gold Nanourchins for Tumor-Targeted Chemo-Photothermal Therapy Integrated with Multimodal Imaging. *Adv. Ther.* **2020**, *3*, 2000114. [[CrossRef](#)]
38. Zhou, J.; Jiang, Y.; Hou, S.; Upputuri, P.K.; Wu, D.; Li, J.; Wang, P.; Zhen, X.; Pramanik, M.; Pu, K.; et al. Compact Plasmonic Blackbody for Cancer Theranosis in the Near-Infrared II Window. *ACS Nano* **2018**, *12*, 2643–2651. [[CrossRef](#)]
39. Kharlamov, A.N.; Feinstein, J.A.; Cramer, J.A.; Boothroyd, J.A.; Shishkina, E.V.; Shur, V. Plasmonic Photothermal Therapy of Atherosclerosis with Nanoparticles: Long-term Outcomes and Safety in NANOM-FIM Trial. *Future Cardiol.* **2017**, *13*, 345–363. [[CrossRef](#)]
40. Kharlamov, A.N. Plasmonic Photothermal Therapy for Atheroregression below Glagov Threshold. *Future Cardiol.* **2013**, *9*, 405–425. [[CrossRef](#)]
41. Singh, P.; Pandit, S.; Mokkapat, V.R.S.S.; Garg, A.; Ravikumar, V.; Mijakovic, I. Gold Nanoparticles in Diagnostics and Therapeutics for Human Cancer. *Int. J. Mol. Sci.* **2018**, *19*, 1979. [[CrossRef](#)] [[PubMed](#)]
42. Bayda, S.; Hadla, M.; Palazzolo, S.; Riello, P.; Corona, G.; Toffoli, G.; Rizzolio, F. Inorganic Nanoparticles for Cancer Therapy: A Transition from Lab to Clinic. *Curr. Med. Chem.* **2018**, *25*, 4269–4303. [[CrossRef](#)] [[PubMed](#)]
43. Kumthekar, P.; Rademaker, A.; Ko, C.; Dixit, K.; Schwartz, M.A.; Sonabend, A.M.; Sharp, L.; Lukas, R.V.; Stupp, R.; Horbinski, C.; et al. A Phase 0 First-in-Human Study Using NU-0129: A Gold base Spherical Nucleic Acid (SNA) Nanoconjugate Targeting BCL2L12 in Recurrent Glioblastoma Patients. *J. Clin. Oncol.* **2019**, *37*, 3012. [[CrossRef](#)]
44. Vucic, S.; Kiernan, M.C.; Menon, P.; Huynh, W.; Rynders, A.; Ho, K.S.; Glanzman, R.; Hotchkiss, M.T. Study Protocol of RESCUE-ALS: A Phase 2, Randomised, Double-blind, Placebo-controlled Study in Early Symptomatic Amyotrophic Lateral Sclerosis Patients to Assess Bioenergetic Catalysis with CNM-Au8 as a Mechanism to Slow Disease Progression. *BMJ Open* **2021**, *11*, e041479. [[CrossRef](#)] [[PubMed](#)]
45. Amal, H.; Leja, M.; Funke, K.; Skapars, R.; Sivins, A.; Ancans, G.; Liepniece-Karele, I.; Kikuste, I.; Lasina, I.; Haick, H. Detection of Precancerous Gastric Lesions and Gastric Cancer through Exhaled Breath. *Gut* **2016**, *65*, 400. [[CrossRef](#)] [[PubMed](#)]
46. Shevtsov, M.; Zhou, Y.; Khachatryan, W.; Multhoff, G.; Gao, H. Recent Advances in Gold Nanoformulations for Cancer Therapy. *Curr. Drug Metab.* **2018**, *19*, 768–780. [[CrossRef](#)]



47. Libutti, S.K.; Paciotti, G.F.; Myer, L.; Haynes, R.; Gannon, W.E., Jr.; Eugeni, M.; Seidel, G.; Shutack, Y.; Yuldasheva, N.; Tamarkin, L. Preliminary Results of a Phase I Clinical Trial of CYT-6091: A PEGylated Colloidal Gold-TNF Nanomedicine. *J. Clin. Oncol.* **2007**, *25*, 3603. [[CrossRef](#)]
48. Libutti, S.K.; Paciotti, G.F.; Byrnes, A.A.; Alexander, H.R., Jr.; Gannon, W.E.; Walker, M.; Seidel, G.D.; Yuldasheva, N.; Tamarkin, L. Phase I and Pharmacokinetic Studies of CYT-6091, A Novel PEGylated Colloidal Gold-rhTNF Nanomedicine. *Clin. Cancer Res.* **2010**, *16*, 6139–6149. [[CrossRef](#)]
49. Zhang, X.D.; Wu, H.Y.; Wu, D.; Wang, Y.Y.; Chang, J.H.; Zhai, Z.B.; Meng, A.M.; Liu, P.X.; Zhang, L.A.; Fan, F.Y. Toxicologic Effects of Gold Nanoparticles In Vivo by Different Administration Routes. *Int. J. Nanomed.* **2010**, *5*, 771–781. [[CrossRef](#)]
50. Nie, S. Understanding and Overcoming Major Barriers in Cancer Nanomedicine. *Nanomedicine* **2010**, *5*, 523–528. [[CrossRef](#)]
51. Lane, L.A.; Qian, X.; Smith, A.M.; Nie, S. Physical Chemistry of Nanomedicine: Understanding the Complex Behaviors of Nanoparticles In Vivo. *Annu. Rev. Phys. Chem.* **2015**, *66*, 521–547. [[CrossRef](#)]
52. Aioub, M.; Kang, B.; Mackey, M.A.; El-Sayed, M.A. Biological Targeting of Plasmonic Nanoparticles Improves Cellular Imaging via the Enhanced Scattering in the Aggregates Formed. *J. Phys. Chem.* **2014**, *5*, 2555–2561. [[CrossRef](#)]
53. Panikkanvalappil, S.R.; Hooshmand, N.; El-Sayed, M.A. Intracellular Assembly of Nuclear-Targeted Gold Nanosphere Enables Selective Plasmonic Photothermal Therapy of Cancer by Shifting Their Absorption Wavelength toward Near-Infrared Region. *Bioconjug. Chem.* **2017**, *28*, 2452–2460. [[CrossRef](#)]
54. Ye, X.; Zheng, C.; Chen, J.; Gao, Y.; Murray, C.B. Using Binary Surfactant Mixtures to Simultaneously Improve the Dimensional Tunability and Monodispersity in the Seeded Growth of Gold Nanorods. *Nano Lett.* **2013**, *13*, 765–771. [[CrossRef](#)]
55. Halas, N. Playing with Plasmons: Tuning the Optical Resonant Properties of Metallic Nanoshells. *MRS Bull.* **2005**, *30*, 362–367. [[CrossRef](#)]
56. Hirsch, L.R.; Stafford, R.J.; Bankson, J.A.; Sershen, S.R.; Rivera, B.; Price, R.E.; Hazle, J.D.; Halas, N.J.; West, J.L. Nanoshell-mediated Near-Infrared Thermal Therapy of Tumors under Magnetic Resonance Guidance. *Proc. Natl. Acad. Sci. USA* **2003**, *100*, 13549–13554. [[CrossRef](#)]
57. Huang, X.; El-Sayed, I.H.; Qian, W.; El-Sayed, M.A. Cancer Cell Imaging and Photothermal Therapy in the Near-Infrared Region by Using Gold Nanorods. *J. Am. Chem. Soc.* **2006**, *128*, 2115–2120. [[CrossRef](#)]
58. An, L.; Wang, Y.; Tian, Q.; Yang, S. Small Gold Nanorods: Recent Advances in Synthesis, Biological Imaging, and Cancer Therapy. *Materials* **2017**, *10*, 1372. [[CrossRef](#)]
59. Chen, H.; Shao, L.; Ming, T.; Sun, Z.; Zhao, C.; Yang, B.; Wang, J. Understanding the Photothermal Conversion Efficiency of Gold Nanocrystals. *Small* **2010**, *6*, 2272–2280. [[CrossRef](#)]
60. Song, J.; Yang, X.; Jacobson, O.; Huang, P.; Sun, X.; Lin, L.; Yan, X.; Niu, G.; Ma, Q.; Chen, X. Ultrasmall Gold Nanorod Vesicles with Enhanced Tumor Accumulation and Fast Excretion from the Body for Cancer Therapy. *Adv. Mater.* **2015**, *27*, 4910–4917. [[CrossRef](#)]
61. Yang, W.; Xia, B.; Wang, L.; Ma, S.; Liang, H.; Wang, D.; Huang, J. Shape Effects of Gold Nanoparticles in Photothermal Cancer Therapy. *Mater. Today Sustain.* **2021**, *13*, 100078. [[CrossRef](#)]
62. Ma, K.; Li, Y.; Wang, Z.; Chen, Y.; Zhang, X.; Chen, C.; Yu, H.; Huang, J.; Yang, Z.; Wang, X.; et al. Core–Shell Gold Nanorod@Layered Double Hydroxide Nanomaterial with Highly Efficient Photothermal Conversion and Its Application in Antibacterial and Tumor Therapy. *ACS Appl. Mater. Interfaces* **2019**, *11*, 29630–29640. [[CrossRef](#)] [[PubMed](#)]
63. Repenko, T.; Rix, A.; Nedilko, A.; Rose, J.; Hermann, A.; Vinokur, R.; Moli, S.; Cao-Milàn, R.; Mayer, M.; von Plessen, G.; et al. Strong Photoacoustic Signal Enhancement by Coating Gold Nanoparticles with Melanin for Biomedical Imaging. *Adv. Funct. Mater.* **2018**, *28*, 1705607. [[CrossRef](#)]
64. Song, J.; Wang, F.; Yang, X.; Ning, B.; Harp, M.G.; Culp, S.H.; Hu, S.; Huang, P.; Nie, L.; Chen, J.; et al. Gold Nanoparticle Coated Carbon Nanotube Ring with Enhanced Raman Scattering and Photothermal Conversion Property for Theranostic Applications. *J. Am. Chem. Soc.* **2016**, *138*, 7005–7015. [[CrossRef](#)]
65. Yang, F.; Zhang, Q.; Huang, S.; Ma, D. Recent Advances of Near Infrared Inorganic Fluorescent Probes for Biomedical Applications. *J. Mater. Chem. B* **2020**, *8*, 7856–7879. [[CrossRef](#)] [[PubMed](#)]
66. Hessel, C.M.; Pattani, V.P.; Rasch, M.; Panthani, M.G.; Koo, B.; Tunnell, J.W.; Korgel, B.A. Copper Selenide Nanocrystals for Photothermal Therapy. *Nano Lett.* **2011**, *11*, 2560–2566. [[CrossRef](#)]
67. Ayala-Orozco, C.; Urban, C.; Knight, M.W.; Urban, A.S.; Neumann, O.; Bishnoi, S.W.; Mukherjee, S.; Goodman, A.M.; Charron, H.; Mitchell, T.; et al. Au Nanomatryoshkas as Efficient Near-Infrared Photothermal Transducers for Cancer Treatment: Benchmarking against Nanoshells. *ACS Nano* **2014**, *8*, 6372–6381. [[CrossRef](#)]
68. Zeng, J.; Goldfeld, D.; Xia, Y. A Plasmon-Assisted Optofluidic (PAOF) System for Measuring the Photothermal Conversion Efficiencies of Gold Nanostructures and Controlling an Electrical Switch. *Angew. Chem. Int. Ed.* **2013**, *52*, 4169–4173. [[CrossRef](#)]
69. Espinosa, A.; Kolosnjaj-Tabi, J.; Abou-Hassan, A.; Plan Sangnier, A.; Curcio, A.; Silva, A.K.A.; Di Corato, R.; Neveu, S.; Pell98egrino, T.; Liz-Marzán, L.M.; et al. Magnetic (Hyper)Thermia or Photothermia? Progressive Comparison of Iron Oxide and Gold Nanoparticles Heating in Water, in Cells, and In Vivo. *Adv. Funct. Mater.* **2018**, *28*, 1803660. [[CrossRef](#)]
70. Gao, F.; Sun, M.; Xu, L.; Liu, L.; Kuang, H.; Xu, C. Biocompatible Cup-Shaped Nanocrystal with Ultrahigh Photothermal Efficiency as Tumor Therapeutic Agent. *Adv. Funct. Mater.* **2017**, *27*, 1700605. [[CrossRef](#)]



71. Ma, N.; Jiang, Y.W.; Zhang, X.; Wu, H.; Myers, J.N.; Liu, P.; Jin, H.; Gu, N.; He, N.; Wu, F.G.; et al. Enhanced Radiosensitization of Gold Nanospikes via Hyperthermia in Combined Cancer Radiation and Photothermal Therapy. *ACS Appl Mater. Interfaces* **2016**, *8*, 28480–28494. [[CrossRef](#)]
72. Huang, P.; Rong, P.; Lin, J.; Li, W.; Yan, X.; Zhang, M.G.; Nie, L.; Niu, G.; Lu, J.; Wang, W.; et al. Triphase Interface Synthesis of Plasmonic Gold Bellflowers as Near-Infrared Light Mediated Acoustic and Thermal Theranostics. *J. Am. Chem. Soc.* **2014**, *136*, 8307–8313. [[CrossRef](#)]
73. Liu, Y.; Zhang, X.; Luo, L.; Li, L.; Zhu, R.Y.; Li, A.; He, Y.; Cao, W.; Niu, K.; Liu, H.; et al. Gold-Nanobranched-Shell based Drug Vehicles with Ultrahigh Photothermal Efficiency for Chemo-Photothermal Therapy. *Nanomedicine* **2019**, *18*, 303–314. [[CrossRef](#)]
74. Chithrani, B.D.; Ghazani, A.A.; Chan, W.C.W. Determining the Size and Shape Dependence of Gold Nanoparticle Uptake into Mammalian Cells. *Nano Lett.* **2006**, *6*, 662–668. [[CrossRef](#)]
75. Chithrani, B.D.; Chan, W.C.W. Elucidating the Mechanism of Cellular Uptake and Removal of Protein-Coated Gold Nanoparticles of Different Sizes and Shapes. *Nano Lett.* **2007**, *7*, 1542–1550. [[CrossRef](#)]
76. Plan Sangnier, A.; Aufaure, R.; Cheong, S.; Motte, L.; Palpant, B.; Tilley, R.D.; Guenin, E.; Wilhelm, C.; Lalatonne, Y. Raspberry-like Small Multicore Gold Nanostructures for Efficient Photothermal Conversion in the First and Second Near-Infrared Windows. *Chem. Commun.* **2019**, *55*, 4055–4058. [[CrossRef](#)]
77. Bi, C.; Chen, J.; Chen, Y.; Song, Y.; Li, A.; Li, S.; Mao, Z.; Gao, C.; Wang, D.; Möhwald, H.; et al. Realizing a Record Photothermal Conversion Efficiency of Spiky Gold Nanoparticles in the Second Near-Infrared Window by Structure-Based Rational Design. *Chem. Mater.* **2018**, *30*, 2709–2718. [[CrossRef](#)]
78. Li, Z.; Li, W.; Camargo, P.H.; Xia, Y. Facile Synthesis of Branched Au Nanostructures by Templating Against a Self-Destructive Lattice of Magnetic Fe Nanoparticles. *Angew. Chem. Int. Ed.* **2008**, *47*, 9653–9656. [[CrossRef](#)]
79. Wang, Z.; Ju, Y.; Tong, S.; Zhang, H.; Lin, J.; Wang, B.; Hou, Y. Au(3)Cu Tetrapod Nanocrystals: Highly Efficient and Metabolizable Multimodality Imaging-Guided NIR-II Photothermal Agents. *Nanoscale Horiz.* **2018**, *3*, 624–631. [[CrossRef](#)]
80. Park, J.E.; Kim, M.; Hwang, J.H.; Nam, J.-M. Golden Opportunities: Plasmonic Gold Nanostructures for Biomedical Applications based on the Second Near-Infrared Window. *Small Methods* **2017**, *1*, 1600032. [[CrossRef](#)]
81. Grzelczak, M.; Sánchez-Iglesias, A.; Rodríguez-González, B.; Alvarez-Puebla, R.; Pérez-Juste, J.; Liz-Marzán, L.M. Influence of Iodide Ions on the Growth of Gold Nanorods: Tuning Tip Curvature and Surface Plasmon Resonance. *Adv. Funct. Mater.* **2008**, *18*, 3780–3786. [[CrossRef](#)]
82. Nam, J.; La, W.G.; Hwang, S.; Ha, Y.S.; Park, N.; Won, N.; Jung, S.; Bhang, S.H.; Ma, Y.J.; Cho, Y.M.; et al. pH-Responsive Assembly of Gold Nanoparticles and “Spatiotemporally Concerted” Drug Release for Synergistic Cancer Therapy. *ACS Nano* **2013**, *7*, 3388–3402. [[CrossRef](#)]
83. Zhang, Y.; Chang, J.; Huang, F.; Yang, L.; Ren, C.; Ma, L.; Zhang, W.; Dong, H.; Liu, J.; Liu, J. Acid-Triggered In Situ Aggregation of Gold Nanoparticles for Multimodal Tumor Imaging and Photothermal Therapy. *ACS Biomater. Sci. Eng.* **2019**, *5*, 1589–1601. [[CrossRef](#)] [[PubMed](#)]
84. Li, S.; Lui, K.H.; Tsoi, T.H.; Lo, W.S.; Li, X.; Hu, X.; Tai, W.C.S.; Hung, C.H.L.; Gu, Y.J.; Wong, W.-T. pH-Responsive Targeted Gold Nanoparticles for In Vivo Photoacoustic Imaging of Tumor Microenvironments. *Nanoscale Adv.* **2019**, *1*, 554–564. [[CrossRef](#)]
85. Isaacson, K.J.; Martin Jensen, M.; Subrahmanyam, N.B.; Ghandehari, H. Matrix-Metalloproteinases as Targets for Controlled Delivery in Cancer: An Analysis of Upregulation and Expression. *J. Control. Release* **2017**, *259*, 62–75. [[CrossRef](#)] [[PubMed](#)]
86. King, S.E. Matrix Metalloproteinases: New Directions toward Inhibition in the Fight Against Cancers. *Future Med. Chem.* **2016**, *8*, 297–309. [[CrossRef](#)] [[PubMed](#)]
87. Jabłońska-Trypuć, A.; Matejczyk, M.; Rosochacki, S. Matrix Metalloproteinases (MMPs), the Main Extracellular Matrix (ECM) Enzymes in Collagen Degradation, as a Target for Anticancer Drugs. *J. Enzyme Inhib. Med. Chem.* **2016**, *31*, 177–183. [[CrossRef](#)] [[PubMed](#)]
88. Yang, K.; Liu, Y.; Wang, Y.; Ren, Q.; Guo, H.; Matson, J.B.; Chen, X.; Nie, Z. Enzyme-Induced In Vivo Assembly of Gold Nanoparticles for Imaging-Guided Synergistic Chemo-Photothermal Therapy of Tumor. *Biomaterials* **2019**, *223*, 119460. [[CrossRef](#)]
89. Ruan, S.; Xiao, W.; Hu, C.; Zhang, H.; Rao, J.; Wang, S.; Wang, X.; He, Q.; Gao, H. Ligand-Mediated and Enzyme-Directed Precise Targeting and Retention for the Enhanced Treatment of Glioblastoma. *ACS Appl. Mater. Interfaces* **2017**, *9*, 20348–20360. [[CrossRef](#)]
90. Cheng, X.; Sun, R.; Yin, L.; Chai, Z.; Shi, H.; Gao, M. Light-Triggered Assembly of Gold Nanoparticles for Photothermal Therapy and Photoacoustic Imaging of Tumors In Vivo. *Adv. Mater.* **2017**, *29*, 1604894. [[CrossRef](#)]
91. Mei, Z.; Gao, D.; Hu, D.; Zhou, H.; Ma, T.; Huang, L.; Liu, X.; Zheng, R.; Zheng, H.; Zhao, P.; et al. Activatable NIR-II Photoacoustic Imaging and Photochemical Synergistic Therapy of MRSA Infections Using Miniature Au/Ag Nanorods. *Biomaterials* **2020**, *251*, 120092. [[CrossRef](#)]
92. Huang, W.; Chen, R.; Peng, Y.; Duan, F.; Huang, Y.; Guo, W.; Chen, X.; Nie, L. In Vivo Quantitative Photoacoustic Diagnosis of Gastric and Intestinal Dysfunctions with a Broad pH-Responsive Sensor. *ACS Nano* **2019**, *13*, 9561–9570. [[CrossRef](#)]
93. Wang, Z.; Zhen, X.; Upputuri, P.K.; Jiang, Y.; Lau, J.; Pramanik, M.; Pu, K.; Xing, B. Redox-Activatable and Acid-Enhanced Nanotheranostics for Second Near-Infrared Photoacoustic Tomography and Combined Photothermal Tumor Therapy. *ACS Nano* **2019**, *13*, 5816–5825. [[CrossRef](#)]
94. Wang, Z.; Upputuri, P.K.; Zhen, X.; Zhang, R.; Jiang, Y.; Ai, X.; Zhang, Z.; Hu, M.; Meng, Z.; Lu, Y.; et al. pH-Sensitive and Biodegradable Charge-Transfer Nanocomplex for Second Near-Infrared Photoacoustic Tumor Imaging. *Nano Res.* **2019**, *12*, 49–55. [[CrossRef](#)]

95. Liu, Y.; Mo, F.; Hu, J.; Jiang, Q.; Wang, X.; Zou, Z.; Zhang, X.Z.; Pang, D.W.; Liu, X. Precision Photothermal Therapy and PhotoAcoustic Imaging by In Situ Activatable Thermoplasmonics. *Chem. Sci.* **2021**, *12*, 10097–10105. [[CrossRef](#)]
96. Ye, J.; Li, Z.; Fu, Q.; Li, Q.; Zhang, X.; Su, L.; Yang, H.; Song, J. Quantitative Photoacoustic Diagnosis and Precise Treatment of Inflammation In Vivo Using Activatable Theranostic Nanoprobe. *Adv. Funct. Mater.* **2020**, *30*, 2001771. [[CrossRef](#)]
97. Sun, M.; Liu, F.; Zhu, Y.; Wang, W.; Hu, J.; Liu, J.; Dai, Z.; Wang, K.; Wei, Y.; Bai, J.; et al. Salt-Induced Aggregation of Gold Nanoparticles for Photoacoustic Imaging and Photothermal Therapy of Cancer. *Nanoscale* **2016**, *8*, 4452–4457. [[CrossRef](#)]
98. Cheng, X.; Zhou, X.; Xu, J.; Sun, R.; Xia, H.; Ding, J.; Chin, Y.E.; Chai, Z.; Shi, H.; Gao, M. Furin enzyme and pH synergistically triggered aggregation of gold nanoparticles for activated photoacoustic imaging and photothermal therapy of tumors. *Anal. Chem.* **2021**, *93*, 9277–9285. [[CrossRef](#)]
99. Ge, X.; Fu, Q.; Su, L.; Li, Z.; Zhang, W.; Chen, T.; Yang, H.; Song, J. Light-Activated Gold Nanorod Vesicles with NIR-II Fluorescence and Photoacoustic Imaging Performances for Cancer Theranostics. *Theranostics* **2020**, *10*, 4809–4821. [[CrossRef](#)]
100. Lin, X.; Liu, S.; Zhang, X.; Zhu, R.; Chen, S.; Chen, X.; Song, J.; Yang, H. An Ultrasound Activated Vesicle of Janus Au-MnO Nanoparticles for Promoted Tumor Penetration and Sono-Chemodynamic Therapy of Orthotopic Liver Cancer. *Angew. Chem. Int. Ed.* **2020**, *59*, 1682–1688. [[CrossRef](#)]
101. Balfourier, A.; Luciani, N.; Wang, G.; Lelong, G.; Ersen, O.; Khelifa, A.; Alloyeau, D.; Gazeau, F.; Carn, F. Unexpected intracellular biodegradation and recrystallization of gold nanoparticles. *Proc. Natl. Acad. Sci. USA* **2020**, *117*, 103–113. [[CrossRef](#)] [[PubMed](#)]
102. Rengan, A.K.; Bukhari, A.B.; Pradhan, A.; Malhotra, R.; Banerjee, R.; Srivastava, R.; De, A. In vivo analysis of biodegradable liposome gold nanoparticles as efficient agents for photothermal therapy of cancer. *Nano Lett.* **2015**, *15*, 842–848. [[CrossRef](#)] [[PubMed](#)]
103. Harima, Y.; Nagata, K.; Harima, K.; Ostapenko, V.V.; Tanaka, Y.; Sawada, S. A Randomized Clinical Trial of Radiation Therapy versus Thermoradiotherapy in Stage IIIB Cervical Carcinoma. *Int. J. Hyperth.* **2001**, *17*, 97–105. [[CrossRef](#)] [[PubMed](#)]
104. Van der Zee, J.; González González, D.; van Rhoon, G.C.; van Dijk, J.D.; van Putten, W.L.; Hart, A.A. Comparison of Radiotherapy alone with Radiotherapy plus Hyperthermia in Locally Advanced Pelvic Tumours: A Prospective, Randomised, Multicentre Trial. Dutch Deep Hyperthermia Group. *Lancet* **2000**, *355*, 1119–1125. [[CrossRef](#)]
105. Zhang, Y.; Zhan, X.; Xiong, J.; Peng, S.; Huang, W.; Joshi, R.; Cai, Y.; Liu, Y.; Li, R.; Yuan, K.; et al. Temperature-Dependent Cell Death Patterns Induced by Functionalized Gold Nanoparticle Photothermal Therapy in Melanoma Cells. *Sci. Rep.* **2018**, *8*, 8720. [[CrossRef](#)]
106. Sweeney, E.E.; Cano-Mejia, J.; Fernandes, R. Photothermal Therapy Generates a Thermal Window of Immunogenic Cell Death in Neuroblastoma. *Small* **2018**, *14*, e1800678. [[CrossRef](#)]